Techno-economic study of chimneyless electric arc furnace plants for the coproduction of steel and of electricity, hydrogen, or methanol

Camilla Nicol Bonacina [a], Matteo Carmelo Romano [a], Paolo Colbertaldo [a], Alessio Milocco [b], Gianluca Valenti [a,*]

[a] *Politecnico di Milano, Dipartimento di Energia, Via Lambruschini 4/a, 20156, Milano, Italy*
[b] *DANIELI & C. OFFICINE MECCANICHE SPA, Via Nazionale, 41, Buttrio, (UD), Italy*

ABSTRACT

Electric arc furnace (EAF) is the most common technology for steel production from steel scrap. Although the input energy is mostly constituted by electricity, significant amounts of carbon dioxide are emitted with the exhaust gases, most of which are classifiable as process-related. The main goal of this study is to perform a techno-economic analysis of chimneyless electric arc furnace plants, fed by either scrap or direct reduced iron (DRI), and able to coproduce steel as well as electricity, hydrogen, or methanol. Several plant configurations are investigated, featuring different combinations of oxy-postcombustion, carbon capture, carbon monoxide-rich gas recovery, hydrogen or syngas production by high-temperature electrolysis or coelectrolysis, and methanol synthesis. These configurations are also characterized by decreased false air leakage and by heat recovery for steam production. Results show that all cases allow achieving a substantial reduction of direct carbon dioxide emissions, close to 99% compared to the unabated conditions. From an economic perspective, in a long-term scenario, the internal rate of return is always above 8%, and up to 73% for the DRI-fed case. However, in a short-term scenario, only cases with sole power production are economically viable. Hydrogen and methanol are competitive with market prices only for low electricity costs. In a higher electricity cost scenario, the case of carbon capture and storage is more competitive than the case of carbon capture and utilization. With an electricity cost of 100 €/MWh, a steel premium of 10–40 €/t allows to reach economic feasibility if methanol or hydrogen selling prices are in line with current market conditions. In general, the configurations with DRI-fed furnaces obtain more favorable economic performance than scrap-fed ones. The competitiveness of sole electricity, hydrogen or methanol production configurations depends on the case study and on the future market prices.

1. Introduction

Steel is the most important engineering and construction material in the world. About 1.9 billion tons of steel are produced worldwide per year (World Steel Association, 2022). The steel industry is highly energy-intensive and is responsible for about 7% of direct carbon dioxide emissions globally. One of the key measures to decarbonize this sector is an increase in the share of steel produced via electric arc furnaces (EAFs). To enable this change, it is particularly important to increase the scrap recycling rate and to set the target of reaching 40% share of the scrap route by 2030 (International Energy Agency, 2021). Also, one of the key measures to decrease the energy consumption in the industrial sector is the implementation of energy saving strategies, such as heat recovery (International Energy Agency, 2019b).

Among the different supply chains for steel production, electric arc furnaces are the most common system for steel waste recycling. The total energy specific consumption and the carbon dioxide specific emission in EAF steelmaking are respectively 1389–4250 kWh/t$_{steel}$, out of which 40–65% is in the form of electricity, and 150-1080 kg$_{CO2}$/t$_{steel}$, most of which are classified as process emissions due to steel liquid decarburization via oxygen injection, electrode graphite consumption, carbon fines injection for slag foaming, and process slag reduction (Kirschen et al., 2009).

Hydrogen is being introduced in the steel industry for mitigating carbon dioxide emissions mainly as substitute of natural gas in the production plants of direct reduced iron (DRI) and pulverized coal injection in blast furnaces, as discussed in (Bailera et al., 2021; Shahabuddin et al., 2023). Other works focus on the utilization of hydrogen as

a fuel, as described in (Marocco et al., 2023). The majority of the literature deals with integrated DRI-EAF systems, as outlined in the work by (Wang et al., 2021) that underlines the dependance of the viability of these plants on the market prices of hydrogen and carbon tax when hydrogen is produced by electrolysis. Additionally, (Andersson and Grönkvist, 2022) integrate the DRI-EAF system with hydrogen electrolysis and methanol production as a storage vector concluding that 25.0% reduction in hydrogen production costs can be achieved assuming historical electricity costs. The use of hydrogen for DRI production has attracted also a great attention in the industry. For example, the large-scale demonstration project HYBRIT aims at producing 2.7 Mt/y of fossil-free DRI (SSAB, L. & V, 2024). In addition, commercial technologies such as ENERGIRON (Danieli, & Tenova, 2024) working with up to 90% of hydrogen have been demonstrated (Shahabuddin et al., 2023). On the other hand, studies and projects about hydrogen utilization and CO_2 mitigation in EAFs are scarce. To the authors' knowledge, the abandoned patent WO2011101217A2 (Waidhas and Wegener, 2011) is the only study addressing the integration of high temperature electrolysis and methanol synthesis from furnace exhaust gas, including in particular EAF.

The scope of this work is to perform a techno-economic study of different plant configurations realizing the novel concept of chimneyless EAF plants, in other words plants in which gases are not emitted ideally to the atmosphere so that chimneys are not present. Specifically, this work considers both EAF plant configurations that use either scrap or DRI as feed. Moreover, these configurations not only produce steel but also, alternatively, electricity, hydrogen, or methanol; they are characterized also by decreased false air leakage and heat recovery for steam production, and optionally: oxy-postcombustion, carbon dioxide capture, carbon monoxide-rich gas recovery, hydrogen or syngas production by high temperature electrolysis or coelectrolysis, and methanol synthesis. Consequently, this work addresses specifically the efficient management of the EAF exhaust gas analyzing different process configurations to fill the gap of studies for the decarbonization of the EAF route in steelmaking processes.

The plant configurations and case studies are presented in Section 2. Section 3 describes the plant units, while Section 4 introduces the economic model. Then, Sections 5, 6 and 7 discuss the results, limits of the study and conclusions, respectively. Finally, additional details on the plants features and the calculation methodology are reported in the supplementary material to this work.

2. Chimneyless plant configurations

Scrap-fed EAF with scrap preheating and DRI-fed EAF are considered as separate case studies due to the different size, mechanical construction, and operation. The new chimneyless processes are characterized by five possible main improvements compared to the state of the art, as follows.

1. Some parts of the EAF itself and the exhaust gas evacuating system are adapted to decrease false air leakage (see also section 3.1).
2. For scrap-fed EAFs, postcombustion of EAF off-gas is performed by oxygen injection, with a recycle stream to control the combustion temperature, generating a CO_2-rich exhaust gas. For DRI-fed EAF, postcombustion is not performed and a CO-rich stream is available in the exhaust gas as a reducing gas for DRI production. The reason behind these different strategies is detailed in section 3.1.
3. A heat recovery system is adopted on the EAF off-gas to produce steam at low-medium pressure, which is used to supply heat to other units, such as carbon capture and methanol purification units, as well as to the electrolysis unit.
4. High-temperature solid oxide electrolysis generates hydrogen or a mixture of hydrogen and carbon monoxide from steam and carbon dioxide.
5. Hydrogen and carbon oxides are converted to methanol.

Fig. 1 shows the block diagram of the plant with its units and potential combinations for scrap- and DRI-fed EAF. The potential combinations and their naming are detailed next and represented in Fig. 2 for sake of clarity.

The scrap-fed EAF has a label starting with 'S', while DRI-fed EAF with 'D'. The scrap- and DRI-fed EAFs have a capacity of 40 and 160 tons of steel per cycle, respectively. The scrap-fed EAF comprises oxy-combustion of CO-rich off-gas. The steam produced from EAF gas heat recovery can be either used for hydrogen or electric energy production. The presence of electrolysis for hydrogen production is depicted with a letter 'H', the sole power production with a letter 'P', and methanol synthesis with a letter 'M', representing the second term of the case study label. Carbon dioxide in scrap-fed EAFs and carbon monoxide in DRI-fed EAFs can be managed in different ways. In the case of scrap-fed EAFs carbon dioxide is stored ('S'), while for DRI-fed EAFs carbon monoxide is recirculated as reducing gas to the DRI production shaft ('R'). When methanol is produced, the cases where hydrogen is produced by steam ('EL') or coelectrolysis ('COEL') are distinguished. Coelectrolysis is adopted in the sole case of scrap-fed furnaces, being the exhaust gas rich in carbon dioxide. All the case studies are compared with the base case studies for scrap- and DRI-fed EAFs available in the market, e.g. without heat recovery, hydrogen and methanol production, as well as carbon dioxide capture. For this reason, the furnace equipment, scrap charging duct, as well as energy and material consumptions of the furnace are not considered in the economic analysis.

3. Plant process and unit models

This section deals first with the electric arc furnace retrofitting and exhaust gas properties. Then, the model of the plant is described briefly. The reader may refer to the supplementary material of this work for additional information about the models of the exhaust gas management unit, of the high-temperature electrolysis and coelectrolysis processes, and of the methanol synthesis plant.

3.1. Electric arc furnace and exhaust gas

Continuous electric arc furnaces can be either fed by scrap or DRI. The former is preheated while being transported in the EAF via a conveyor by the exhaust gas flowing in countercurrent, as in state-of-the-art technology. The latter is introduced at high temperature directly from the top of the EAF. The EAF can be retrofitted to avoid air leakages in different points as follows.

- for electrodes, abradable seals and a hermetic shell-compensation chamber dynamic sealing system are used;
- the EAF upper shell is closed through the construction of metal sheets to avoid air leakages below the support point of cooling panels;
- the slag door is substituted with a zero-leakage door (such as Danieli's *THOR 3k®* door equipped with sealing and mechanic cleaning devices that maintain a constant slag level to seal the door);
- a sealing mechanism is designed in the exhaust gas exit section;
- oxygen lances are substituted by oxygen injectors, which remain always in the same position instead of moving from the EAF upper shell avoiding air leakages;
- the charging scrap conveyor is modified in order to decrease air leakages through mechanical devices.

Thanks to these strategies, a nitrogen fraction between just 5% and 10% is expected to leak into the EAF. The trends of the expected exhaust gas flow rate, composition, and temperature profiles with decreased air leakage have been computed with a Danieli in-house model. Fig. 3 summarizes the exhaust gas volume flow rates, composition, and temperatures over the whole tap-to-tap time during power-on for scrap- and DRI-fed EAFs. Table 1 depicts the properties of the gas used as input to the process model developed within the Aspen Plus environment, which
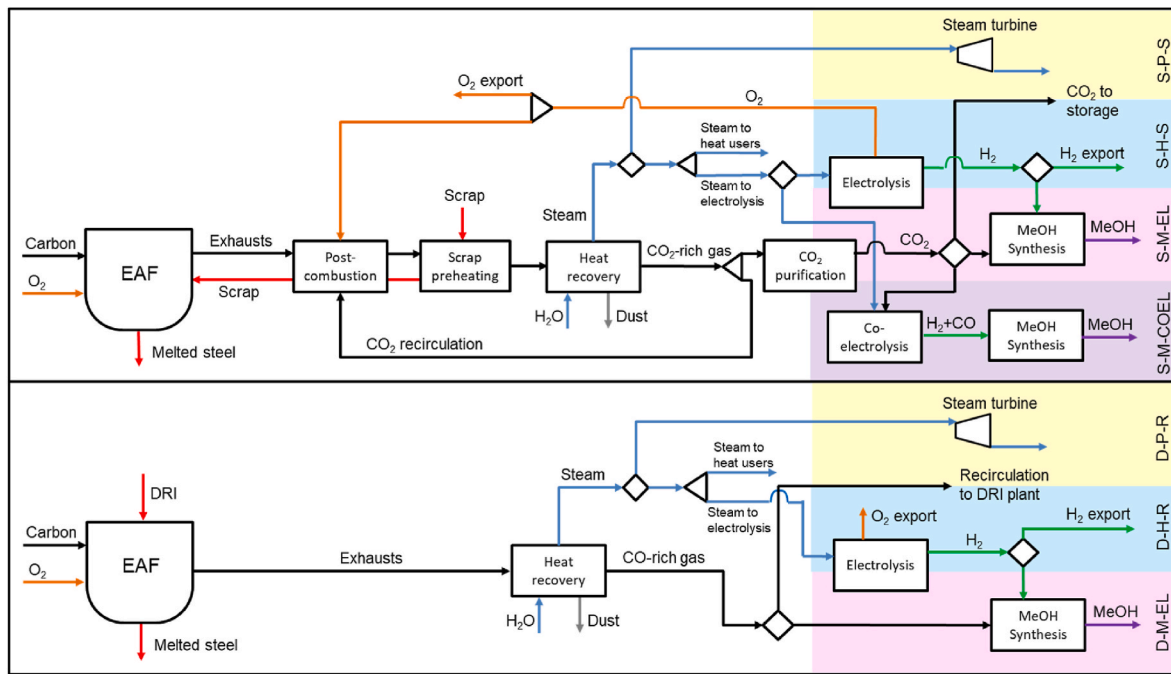
Fig. 1. Block diagram of the potential configurations of the plant for scrap- (top) and DRI-fed (bottom) EAFs comprised of heat recovery, and gas treatment unit, and optionally oxy-combustion, electrolysis and methanol synthesis. A diamond block is used to represent the alternative stream potential routes.
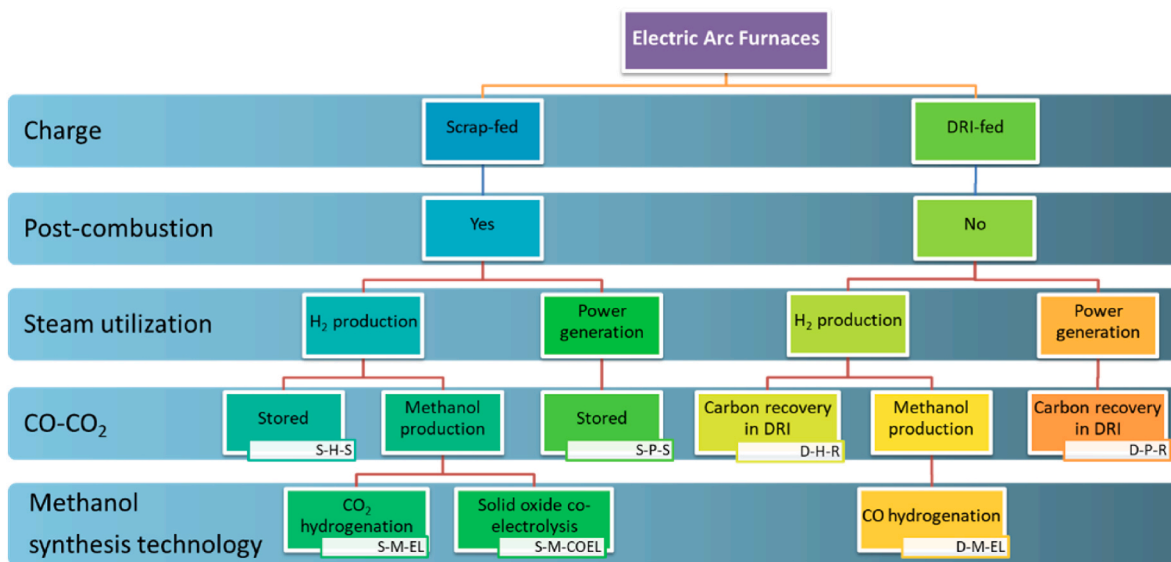

Fig. 2. Case studies and naming. The first term in the name code refers to the source of iron for the EAF, which can be either scrap ('S') or DRI ('D'). The second term represents the presence of sole hydrogen production ('H'), sole power production ('P'), or methanol synthesis ('M') fed either by hydrogen from steam electrolysis ('EL') or by H_2O–CO_2 coelectrolysis ('COEL'). When methanol is not produced, CO_2 is stored ('S') in scrap-fed EAF plants, or the CO-rich gas is recirculated to the DRI production shaft ('R') in the DRI-fed EAF.

is the commercial software employed in this work. These gas properties are expressed as average values over the entire tap-to-tap time span. The steady-state calculation approach with average gas properties involves the presence of a gas holder for buffering the flow rate variations and a steam drum boiler for thermal storage.

The careful management of the CO-rich gas is fundamental when air leakages are limited due to its potential explosions inside the exhaust gas evacuation ducts, especially for scrap-fed EAFs where these leakages cannot be completely avoided due to the mechanical construction of the scrap charging conveyor itself. Postcombustion by oxygen can be performed to solve this issue, while facilitating carbon capture. Air

separation units (ASUs) are already present in steelmaking plants, and additional oxygen can be produced by electrolysis. Thus, post-combustion is performed for scrap-fed EAFs via simple oxygen injection, while flue gas recirculation is adopted to prevent excessive temperatures in the postcombustion zones, i.e. remain below 1600 °C. For DRI-fed EAFs, postcombustion is not performed because of the absence of the charging duct and of the possibility to avoid air leakages and uncontrolled explosions of carbon monoxide outside the furnace, while assuming that all the oxygen in the leaked air burns a portion of carbon monoxide; this allows recovering the CO-rich gas either for methanol synthesis or as reducing gas in the DRI production shaft. This approach is
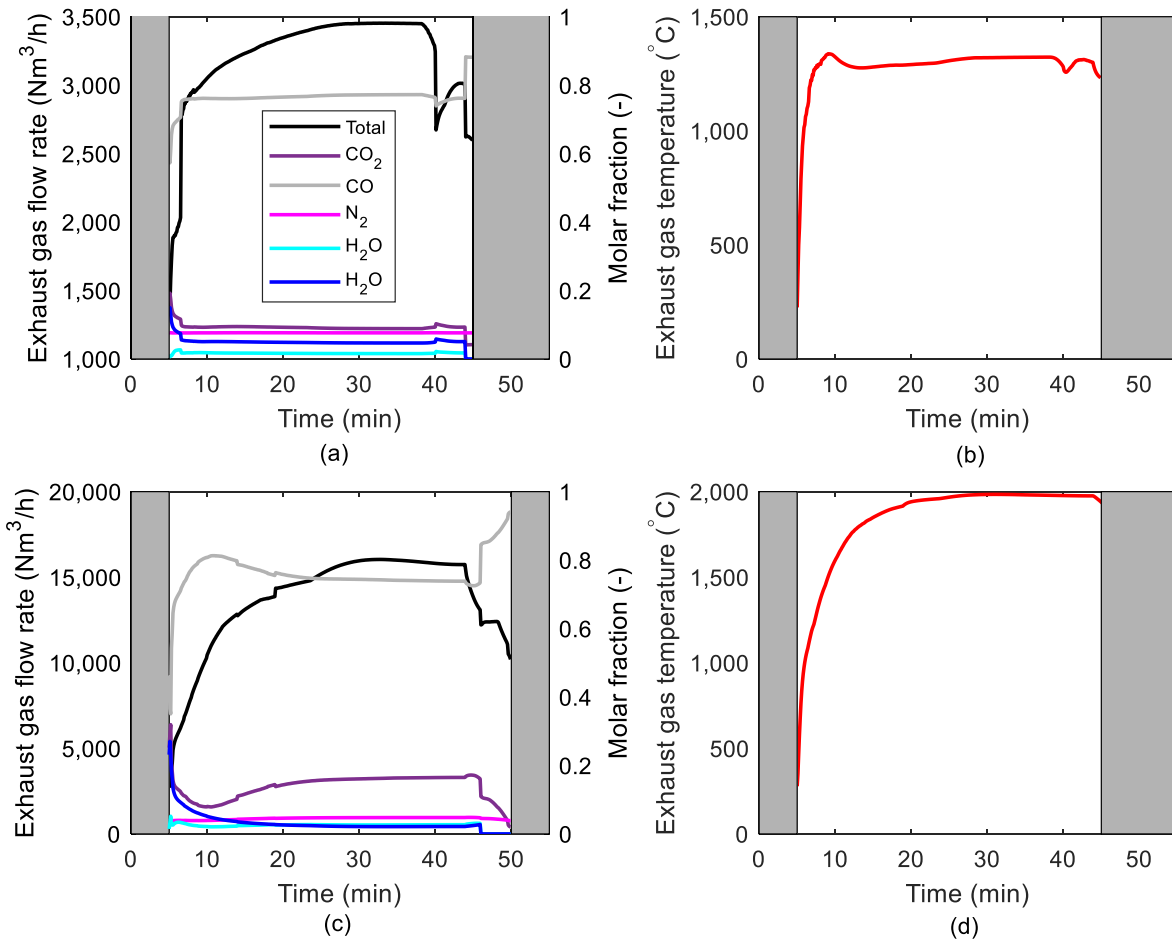
Fig. 3. Exhaust gas flow rate, composition, and temperature profiles in scrap-fed (a and b) and DRI-fed (c and d) furnace. Grey areas represent the power-off time.

Table 1

Main exhaust gas properties used as input parameters in process model developed within the Aspen Plus environment, the commercial software used in this work. These gas properties are expressed as average values over the entire tap-to-tap time span.

Parameter	Unit	Scrap 40 tons	DRI 160 tons
Volumetric flow rate	Nm^3/h	2328	11,199
CO_2 molar fraction	%	9.25	13.79
CO molar fraction	%	76.48	76.20
N_2 molar fraction	%	7.65	4.52
H_2O molar fraction	%	1.66	2.40
H_2 fraction	%	4.97	3.09
Temperature	°C	1283	1838
CO_2 produced by EAF	kg/t_{steel}	98	124
	kt/year	29	147

a simplification of the real conditions of the furnace, where small air leakages in cold spots of the duct may lead to the coexistence of O_2 and CO.

3.2. Heat recovery unit

For heat recovery, a system similar to 'Waste to Heat' plants is used in all the case studies of the present work with the scope of producing steam from the thermal power in the EAF exhausts. Water-tube bundles for water preheating, evaporation, and steam superheating are considered. At the same time, gas treatment is performed with the aid of a settling chamber and a high-temperature filter located after the evaporator, at around 600 °C, and after the superheater, at around 380 °C,

respectively. Superheated steam can be expanded in a turbine for power generation with an assumed efficiency of 70%. Depending on whether electrolysis is performed or not, back-pressure or condensing turbines are selected. The live steam pressure and temperature at turbine inlet are 28 bar and 400 °C. The condensing pressure is set equal to 0.05 bar. A heat pump with a coefficient of performance equal to 2 is considered to provide the thermal power input that cannot be provided through heat integration, such as the demand from the methanol distillation column, when present, and from the feedwater pre-heating. A plant temperature-
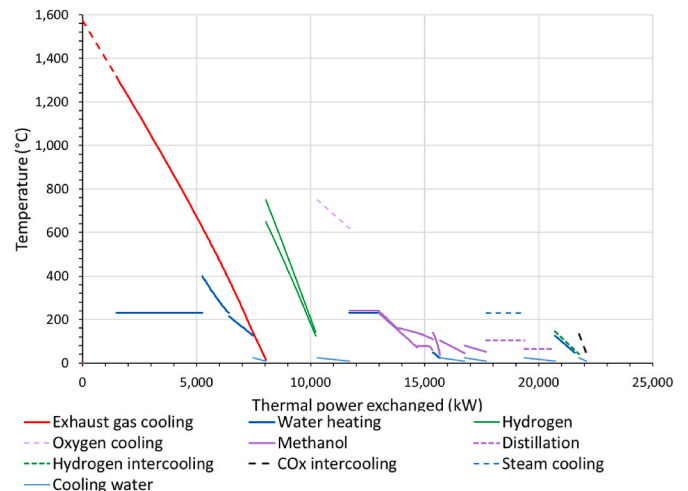

Fig. 4. Temperature-exchanged thermal power diagram for the case S-M-EL.

heat diagram is reported in Fig. 4 for the illustrative case S-M-EL. The reader may refer to the supplementary material for further details about the heat recovery model.

3.3. High-temperature electrolysis

Steam generated via heat recovery could be efficiently split into hydrogen and oxygen in a solid oxide electrolysis (SOEC) system. Hydrogen can be used for methanol synthesis and/or directly in the steelmaking plant as a fuel. Oxygen can also be recovered and used in the EAF. The high-temperature electrolyzer can also work in coelectrolysis mode producing a H_2–CO mixture (Smolinka et al., 2015). When methanol synthesis is performed, the carbon dioxide and the steam feed are controlled to obtain a methanol feed stoichiometric module of 2.05. When methanol synthesis is not performed, the electrolyzer is sized on the steam produced from heat recovery, while the whole hydrogen produced is either exported as a byproduct or used in other processes of the steel plant. For the purpose of this work, the electrolyzer is assumed to operate at 1 bar and 750 °C, with a steam utilization factor of 75% and a hydrogen recycle ratio of 10%$_{vol}$. The operating voltage is kept above the thermo-neutral value to allow exothermic operation, thus avoiding additional high-temperature heat supply. Voltage values vary between the electrolysis and coelectrolysis cases. The reader may refer to the supplementary material of this work for further details about the high-temperature electrolysis model.

3.4. Methanol production

After heat recovery in the scrap-fed furnaces, carbon dioxide is either captured or used for methanol synthesis. In the former case, purification is performed. Due to the high concentrations of carbon dioxide, the purification unit is carried out with low-temperature phase-change process, recovering 96% of high-purity, as high as 99.99%, carbon dioxide with an electricity consumption of 130 kWh/t$_{CO2}$ (Magli et al., 2022). In the DRI-fed EAF cases, after heat recovery, carbon monoxide is either directly recovered to the DRI production shaft or used for the methanol production. The synthesis process is based on a Lurgi boiling water reactor operating at 90 bar and 240 °C with equilibrium outlet composition. The purge ratio from the methanol loop is set to 1%. Methanol is purified in a two-column process, achieving methanol purity of around 99.1% and water purity of 99.9%. The reader may refer to the supplementary material of this work for further details about the methanol synthesis model.

4. Economic model

This chapter deals with the economic model for all configurations. The economic performance indicators considered in this study are the internal rate of return *IRR* (%), the levelized cost of hydrogen *LCOH* (€/kg), and that of methanol *LCOM* (€/kg). The *IRR* (%) is computed as the value of the discount rate r (−) that makes the net present value *NPV* (€) equal to zero in the following:

$$NPV = - C_{inv} + \sum_{t=1}^{LT} \frac{NCF}{(1+r)^t} \quad (1)$$

where C_{inv} (€) is the total investment cost, *NCF* (€/y) is the annual net cash flow, assumed constant throughout the years, and *LT* (years) is the plant lifetime. The levelized cost of hydrogen and methanol, expressed generically as *LCOX* (€/kg), are calculated following a procedure similar to that applied by Minutillo et al. (2021) for hydrogen, as follows:

$$LCOX = \frac{\sum C_{inv,y} + \sum C_{O\&M} + NCF}{\dot{m}_{i,y}} \quad (2)$$

where $\dot{m}_{i,y}$ (kg/year) is the total amount of hydrogen or methanol pro-

duced in a year, and $C_{inv,i,y}$ (€/y) is the annualized investment cost.

In its turn, the annualized investment cost, $C_{inv,y}$ (€/y), is calculated assuming that the investment occurs fully at the beginning of the project, as follows:

$$C_{inv,y} = C_{inv} \frac{r(1+r)^{LT}}{(1+r)^{LT} - 1} \quad (3)$$

The total investment cost is calculated as the sum of the investment cost of the active units in the plant. The investment cost of each unit 'i' is calculated as:

$$C_{inv,i} = EC_i(1+ICF)(1+CF) \quad (4)$$

where EC_i (€) is the equipment cost, *ICF* (−) the installation cost factor assumed equal to 70% (Gatti et al., 2020), and *CF* (−) the cost factor including indirect, owner's, and contingency costs assumed equal to 75% (Blumberg et al., 2019). The equipment costs of heat recovery, methanol synthesis, and CO_2 capture are scaled according to the following cost function:

$$EC = EC_{ref}\left(\frac{S}{S_{ref}}\right)^P \quad (5)$$

where EC_{ref} (€) is the reference equipment cost, S the size of the equipment, S_{ref} the reference equipment size, and P (−) the scaling factor. The reference costs are reported to year 2021 by the CEPCI index (Chemical Engineering, 2024). Additionally, the cost of electrolysis stack replacement at year 10, given by $C_{rep,EL,t=10}$ (€), is actualized to year 0 in the term $C_{rep,EL}$ (€) following the procedure presented in (Crespi et al., 2021):

$$C_{rep,EL} = \frac{C_{rep,EL,t=10}}{(1+r)^{10}} \quad (6)$$

Moreover, the net cash flows *NCF* (€/y) are calculated considering the annual revenues R (€/y), the variable costs C_{var} (€/y), and the annual fixed costs for operation and maintenance $C_{O\&M}$ (€/y) as:

$$NCF = R - C_{var} - C_{O\&M} \quad (7)$$

where the revenues consider the hydrogen and methanol sale as well as the avoided costs, i.e. carbon tax and avoided oxygen production consumptions. The selling price of hydrogen is assumed between 3 and 5 €/kg, considering low-carbon hydrogen levelized cost in 2019 in the range 3.2–7.7 €/kg, and expected low-carbon hydrogen levelized cost by 2060 in the range 1.3–3.3 €/kg (International Energy Agency, 2019a). The selling price of methanol is assumed between 400 and 500 €/kg according to current medium price ranges in the market (Methanol Institute, 2024).The carbon tax avoided cost considers the CO_2 emissions to the atmosphere from the EAF exhaust gas of the conventional plant. The cash flow associated with oxygen import/export is computed considering electricity consumption for oxygen production in a cryogenic ASU of 247 kWh/t$_{O2}$ (Hong et al., 2009). The additional revenue due to the possible application of a premium on the sale of decarbonized steel is not considered in this analysis to obtain conservative results.

The variable costs C_{var} (€/y) are calculated as follows:

$$C_{var} = \dot{W}_{el} \bullet P_{el} \bullet H + C_{carbon} \quad (8)$$

where $\dot{W}_{el}$ (MW) is the net electric power input, P_{el} (€/MWh) is the electricity cost for steelmaking users, H (h/y) the hours of operation of the plant in a year. C_{carbon} (€/y) are the costs related to the management of carbon dioxide either captured in the plant in scrap-fed EAF cases or additionally produced in DRI production facilities when carbon monoxide is recovered in DRI-fed EAF as depicted in the next section. These CO_2 management costs include transport and geological storage, excluding the capture and purification phase that is accounted for separately. Table 2 and Table 3 list the parameters adopted to calculate

Table 2
Parameters for calculating the equipment costs. The electrolysis and methanol costs comprise installation costs. The CO_2 purification cost comprises installation and indirect costs. As the methanol plant includes the cost of CO_2 compression, when methanol synthesis is performed, the costs of CO_2 purification are reduced by 33.9% to avoid accounting for compression equipment costs in both methanol and CO_2 purification units in the final compression stage (CLEANKER, 2017). Scaling factors are retrieved from (Gatti et al., 2020) for the heat recovery system, and from (Pratschner et al., 2023) for the methanol and carbon dioxide purification unit.

Component	Scaling parameter	Reference size	Reference cost	Reference	Scaling factor
Electrolysis	–	–	500-1000 €/kW$_{el}$	Clean Air Task Force (2023)	–
Heat exchangers	UA	10.06 MW$_{th}$/K	31.6 M€$_{2014}$	Gatti et al. (2020)	0.67
Steam turbine	Electric power	293.2 MW$_{el}$	49.0 M€$_{2014}$	Gatti et al. (2020)	0.67
Cooling water	Thermal power	436.6 MW$_{th}$	15.5 M€$_{2014}$	Gatti et al. (2020)	0.67
Methanol plant	Methanol produced	2803 t/d	80.64 M€$_{2016}$	Blumberg et al. (2019)	0.8
CO_2 purification	CO_2 purified	120 t/h	46.09 M€$_{2018}$	Magli et al. (2022)	0.65
Heat pump	Electric power	500 kW	250 €/kW$_{2021}$	Arpagaus (2021)	0.67

Table 3
Main assumptions for the economic analysis.

Parameter	Unit	Value
Electricity purchasing price	€/MWh	50–100
O_2 production consumption	kWh/t$_{O2}$	247 (Hong et al., 2009)
Hydrogen selling price	€/kg$_{H2}$	3–5
Methanol selling price	€/t$_{MeOH}$	400–500
Carbon tax	€/t$_{CO2}$	100
CO-rich gas value[a]	€/GJ$_{LHV}$	−5.9
Hours of operation	h/year	7440
Discount rate	%	8
Plant lifetime	years	20
Electrolysis unit lifetime	years	10
Electrolysis stack replacement	% of $C_{inv,EL}$	40
CO_2 management cost[b]	€/t$_{CO2}$	30
Operation and maintenance	% of C_{inv}/year	2
Installation cost factor[c]	%	70 (Gatti et al., 2020)
Indirect cost factor[d]	%	75

[a] The economic value of the CO-rich gas exported to the DRI plant is evaluated with a simplified approach assuming to feed a NG based DRI plant and considering: (i) the saved natural gas (having a cost of 9 €/GJ$_{LHV}$), calculated from the relative reducing potential of CO and CH_4 and (ii) the additional CO_2 generated from CO oxidation (having a cost of emission or management of the CO_2 of 100 €/t$_{CO2}$). The reader is addressed to the supplementary information for a complete discussion of the calculation method. The CO-rich gas value results to be negative, as the cost of CO_2 emission/management results higher than the limited saved cost of natural gas consumption.
[b] The assumed cost for CO_2 transport and storage is an intermediate value between around 10 €/t, representative of pipelines transport (Rubin et al., 2015), and 50 €/t, representative of transport by ships over long distances (d'Amore et al., 2024).
[c] Installation costs of electrolysis, methanol and carbon purification units are included in the reference costs of Table 2.
[d] Indirect costs of carbon purification unit are included in the reference costs of Table 2.

the equipment costs and the main assumptions for the economic analysis, respectively.

5. Results and discussion

This section describes and discusses the results of this study from a technical and economic point of view.

5.1. Technical analysis

The main technical results of the assessed cases are reported in Table 4. In all cases with methanol production, steam production is higher than in the cases without methanol production. This is due to the steam generated in the water-cooled methanol reactor. The electrolysis island consumes around 90% and 99% of the total electricity demand in the cases with methanol and hydrogen production, respectively. In the case S–P–S, electricity is consumed mainly in the carbon capture and

compression section and balanced by the power generated by the steam turbine, which leads to nearly electric neutral cases. The overall thermal power rejected to ambient is negligible with respect to the total heat exchanged thanks to heat integration strategies, and it is mainly associated to the cooling duty in the methanol and hydrogen units as well as in the steam cycle condenser, when present.

In the case S–H–S, the generated steam determines the size of the electrolysis plant, as all the steam is used for hydrogen production. This is the reason why this case has higher electricity consumptions than the S-M-EL and S-M-COEL cases, where the SOEC capacity is determined by the amount of carbon oxides to be converted into methanol and the excess steam is used within the plant for heating purposes. Conversely, in the DRI-fed EAF, the electric consumption of the D-H-R case is lower than the D-M-EL case because the absence of postcombustion reduces the relative amount of thermal power available in the EAF gas. In all cases with hydrogen and methanol production, oxygen produced by electrolysis is higher than that consumed for postcombustion, making it possible to export oxygen for other uses in the steel plant. The methanol production capacities for the scrap- and DRI-fed EAFs are about 66 tpd and 355 tpd, respectively. These values correspond to half and three times the capacity of the e-methanol North-C production plant, equal to 123 tpd, that is planned as a carbon capture and utilization (CCU) demonstrator (N.C. Hub, 2024); furthermore, the values are 1 and 2 orders of magnitude smaller than the 2500 tpd capacity of the largest conventional natural gas-based methanol plant in Europe (TBU, 2024).

In addition, Table 4 reports the CO_2 balance associated to CO-rich gas recovery in the DRI plant, showing the amount of carbon dioxide (i) produced by the CO-rich gas, (ii) avoided from the equivalent saved amount of natural gas as a reducing agent, and (iii) the net balance resulting from the above-mentioned contributions. The reader may refer to the supplementary material of this work for a simplified scheme of carbon balances of the DRI-EAF system.

Table 5 shows the main energy input and stream products per ton of tapped steel. The specific net electric power input is between 235 and 649 kWh/t$_{steel}$ when hydrogen or methanol are produced. These values have the same order of magnitude as the electricity consumption in the EAF steel melting process considered in this case study, which is about 350 kWh/t$_{steel}$. In the power production cases, an electric energy saving of 12–13 kWh/t$_{steel}$ is attained. Still referring to Table 5, the specific net electric power input for the DRI-fed cases is lower than for the scrap-fed cases, due to the absence of postcombustion, which leads to a CO-rich feed to the methanol island, in turn lowering the hydrogen needed to convert carbon to methanol. This can also be noticed by the net electric power input specific to the amount of methanol produced, which is lower for the DRI-fed EAF case. This is consistent with the findings by (d'Amore et al., 2023) about the advantages related to the direct conversion of carbon monoxide rather than carbon dioxide, when technically feasible. The table shows also the methanol, hydrogen, and oxygen export together with the CO_2 and CO mass balances. In all case studies, carbon dioxide emissions are maintained below 1.1 kg/t$_{steel}$, leading to a substantial reduction of direct carbon dioxide emissions always above

Table 4

Technical results of the plant in the different configurations, comprising the overall power and mass balances, as well as heat recovery, electrolysis and methanol synthesis island results.

Parameter	Unit	S-M-EL	S–H–S	S–P–S	S-M-COEL	D-M-EL	D-H-R	D-P-R
Power balance								
Net electric power input	MW	20.80	23.78	−0.44	19.37	79.23	33.87	−1.89
Electric power input	MW	22.11	24.86	1.34	20.77	82.68	35.47	0.74
Heat recovery fan and pump	MW	0.02	0.02	0.03	0.03	0.04	0.02	0.03
Heat pump	MW	0.00	0.48	0.48	0.00	3.87	0.72	0.72
Electrolysis	MW	20.57	24.82		19.39	74.96	36.67	
CO_2 purification	MW	0.48	0.48	0.48	0.48			
Methanol synthesis	MW	1.75			1.53	7.73		
Oxygen consumption	MW	−0.73	−0.95	0.35	−0.67	−3.92	−1.94	
Steam turbine power output	MW	1.31	1.08	1.78	1.40	3.46	1.60	2.64
Heat rejected to ambient	MW	3.44	0.61	5.65	3.33	15.19	0.76	8.24
Mass balance								
Methanol export	kg/h	2662			2686	14,253		
	MW	14.71			14.85	78.79		
Hydrogen export	kg/h		670				993	
	MW		22.33				33.11	
O_2 export	kg/h	2938	3852	−1421	2716	15,851	7849	
CO_2 captured for storage	kg/h		3719	3719				
CO-rich gas export	$kg_{CO\text{-}rich}$/h						14,574	14,574
	$MW_{CO\text{-}rich}$						32.72	32.72
	kg_{CO2}/h						19,784	19,784
NG and CO_2 savings from CO-rich gas export	kg_{NGeq}/h						1649	1649
	MW_{NGeq}						22.91	22.91
	kg_{CO2}/h						4535	4535
Net CO_2 generated from CO-rich gas export	kg_{CO2}/h						15,248	15,248
Heat recovery island								
Produced steam	kg/h	9687	7985	7985	10,341	25,610	11,841	11,841
Consumed oxygen	kg/h	1421	1421	1421	1421			
Thermal power recovered	MW	7.29	6.01	6.01	7.78	19.27	8.91	8.91
Electrolysis island								
Produced hydrogen	kg/h	520	670		423	1966	993	
Produced oxygen	kg/h	4359	5273		4138	15,851	7849	
Stack efficiency (LHV)	–	0.896	0.898		1.090	0.895	0.903	
Current density	A/cm^2	0.677	0.677		0.784	0.677	0.677	
Voltage	V	1.370	1.370		1.391	1.370	1.370	
Methanol synthesis island								
Tail gas combustion power	MW	0.66			0.62	2.97		
Thermal power input	MW	1.68			1.47	8.79		
Heat rejected to ambient	MW	2.81			2.35	14.29		
Recycle ratio (RR)	–	2.61			2.68	3.91		
Carbon efficiency	%	97.7			98.3	98.3		
Methanol purity	%mass	99.4			99.1	99.4		
Water purity	%mass	99.9			999	99.9		

Table 5

Main energy input and stream products per ton of tapped steel.

Parameter	Unit	S-M-EL	S–H–S	S–P–S	S-M-COEL	D-M-EL	D-H-R	D-P-R
Net electric power input	kWh/t_{steel}	567.31	648.57	−11.90	528.26	550.19	235.21	−13.16
	kWh/$t_{MeOH/H2}$	7.8	35.5		7.2	5.6	34.1	
Methanol export	kg/t_{steel}	72.6			73.3	99.0		
Hydrogen export	kg/t_{steel}		18.3				6.9	
Oxygen export	kg/t_{steel}	80.1	105.1	−38.8	74.1	110.1	54.5	
CO_2 emitted	kg/t_{steel}	1.1	0.0	0.0	0.7	0.8	0.0	0.0
CO_2 stored	kg/t_{steel}		101.4	101.4			137.4[a]	137.4[a]
CO_2 converted	kg/t_{steel}	100.3			100.7	136.6		
CO recovered	kg/t_{steel}						74.0	74.0
Produced steam	kg/t_{steel}	264.2	217.8	217.8	282.0	177.8	82.2	82.2

[a] includes 21.1 kg/t_{steel} of CO_2 exported with the EAF off-gas +116.3 kg/t_{steel} of CO_2 generated by CO oxidation in the DRI plant.

99%.

To validate the obtained results, some significant quantities, which are reported in Table 6, are compared to literature ones. For the electrolysis unit, the specific electric energy consumption is around 35 kWh/t_{H2}, which is comparable to declared values of Sunfire's commercial cells (Sunfire, 2024). For the methanol synthesis unit in the scrap-fed case, overall carbon dioxide conversion is of about 1.4 t_{CO2}/t_{MeOH}, i.e. close to the stoichiometric ratio, which is in agreement with (Pérez-Fortes et al., 2016; Leonzio et al., 2019; Kiss et al., 2016). Carbon efficiency, i.e. the

Table 6

Parameters used for validation of the overall plant technical results.

Parameter	Unit	Value
Solid oxide electrolysis specific energy consumption	kWh/t_{H2}	35
Methanol synthesis CO_2 conversion	t_{CO2}/t_{MeOH}	1.4
Methanol synthesis carbon efficiency	%	97.7–98.3
Methanol synthesis specific energy consumption[a]	GJ$_e$/t_{MeOH}	30

[a] referred to case study S-M-EL and S-M-COEL.

carbon in the methanol product with respect to the carbon in the methanol island feed, is between 97.7% and 98.3%, which is consistent with the values reported by (Kiss et al., 2016). Ultimately, the specific electricity consumptions are in agreement with 30 GJ_e/t_{MeOH} (i.e. 8.3 kWh/t_{MeOH}) calculated for a system based on high-temperature electrolysis by (Abad et al., 2021).

5.2. Economic analysis

To evaluate the economics of the plant, two scenarios are considered. In the long-term scenario, electrolyzer investment cost is 500 €/kW_{el}, electricity cost is 50 €/MWh, and hydrogen and methanol selling prices are 5 €/kg and 500 €/t. In the short-term scenario, instead, electrolyzer investment cost is 1000 €/kW_{el}, electricity cost is 100 €/MWh, and hydrogen and methanol selling prices are 3 €/kg and 400 €/t. The main costs and revenues of the different cases are depicted in Table 7, for the long-term scenario, and Table 8, short-term one. The DRI-fed EAF cases are more competitive than the scrap-fed EAF ones due to both the more efficient methanol synthesis and the absence of carbon capture costs. Electrolysis, when present, represents the highest cost share, while in case S–P–S the main costs are related to carbon capture. The effect of electricity cost on the viability of the case study is significant. Indeed, almost none of the scrap-fed EAF cases is competitive in the short-term scenario, when the electricity cost is 100 €/MWh. In the long-term scenario, the *IRR* varies between 8 and 45% for scrap-fed EAF cases and between 29 and 73% in DRI-fed EAF cases when hydrogen or methanol are produced. In the short-term scenario, only case studies S–P–S, D-H-R, and D-P-R result to be competitive, with an *IRR* of 9%, 2%, and 78%, respectively. The competitiveness of case studies S–P–S and D-P-R is not affected considerably by the scenario assumptions because the net electricity production is small. Interestingly, in all cases the revenues from hydrogen and methanol sale, up to 25 M€/y in the scrap cases and up to 53 M€/y in the DRI cases, are much lower than the revenues from steel sale, which would be equal to 162 and 662 M€/y in the scrap- and DRI-fed EAF cases, respectively, considering a sale price of 500 €/t_{steel}. Therefore, hydrogen and methanol can be considered as byproducts of the steel production process, letting steel remain the main source of revenues of the plants.

Figs. 5 and 6 show the hydrogen and methanol selling price breakeven line and iso-*IRR* lines for fixed electrolyzer and electricity costs. The breakeven line represents the product selling price that makes the net present value equal to zero, and identifies the regions that make hydrogen production more competitive, in the region above the line, or methanol production more competitive, below the line. In Fig. 5, the competitiveness of cases S-M-EL and S–H–S is shown. The same chart is repeated in Fig. 6 for cases D-M-EL and D-H-R. The results are presented for two cases with an electrolyzer cost and electricity cost of (a) 1000 €/kW and 100 €/MWh, and (b) 500 €/kW and 50 €/MWh, respectively. Case S-M-COEL is not reported in these charts, as results are very similar to case S-M-EL.

In the scrap-fed EAF cases, hydrogen and methanol production is competitive with respect to the identified selling price range (see Table 3) only for low electricity costs. The same is observed in the DRI-fed cases. Overall, these charts confirm the higher competitivity of DRI-fed EAF configurations, which show better *IRR* for given methanol and hydrogen prices with respect to the scrap-fed EAF cases. It is interesting to note that in all cases, the breakeven line corresponds to points with methanol to hydrogen price ratio in the relatively narrow range of 170–250 (€/t_{MeOH})/(€/kg_{H2}). This indicates that the relative competitivity between methanol and hydrogen production is mildly influenced by the SOEC capex and the electricity cost.

Fig. 7 shows the carbon management cost and methanol selling price breakeven line to identify whether case S–P–S, in the region below the line, or S-M-EL, above the line, is more competitive. This chart allows a comparison between carbon capture and storage (CCS) and carbon capture and utilization (CCU) options. As expected, high electricity costs tend to favor the CCS case with respect to the CCU case. In the higher electricity cost scenario (Fig. 7a), with methanol selling price below 600 €/t_{MeOH}, the CCS S–P–S case is more competitive than the CCU S-M-EL case, except for extremely high carbon management costs, above 100 €/t_{CO2}. In the low electricity cost scenario (Fig. 7b), with a methanol selling price of 500 €/t_{MeOH}, the CCU S-M-EL case results to be more competitive than the CCS S–P–S case for relatively high carbon management costs, above 40 €/t_{CO2}.

In short, the novel proposed chimneyless electric arc furnaces appear to be economically promising options to reduce carbon dioxide emissions especially in the DRI-fed cases, and the competitiveness of the electricity, hydrogen, or methanol production configurations depends on the case study analyzed and, especially, on the relative market prices of methanol, hydrogen and cost of CO_2 transport and storage.

Regarding the net present value analysis, Fig. 8 illustrates the steel premium and methanol price that set the *NPV* to zero for a fixed electricity cost with an electrolyzer cost of 1000 €/kW_{el} and for cases S-M-EL and D-M-EL. At a fixed steel premium, the breakeven methanol price (i. e. leading to *NPV* = 0) increases with higher electricity price with a linear trend. The case in which the steel premium is zero corresponds to the cases previously analyzed. Similar considerations can be drawn from Fig. 9, which shows similar trends for hydrogen production cases S–H–S and D-H-R.

Fig. 8 depicts that for a breakeven methanol selling price of 400 €/t, a

Table 7
Costs and revenues of the different case studies for the long-term scenario, with an electrolyzer investment cost of 500 €/kW_{el}, an electricity cost of 50 €/MWh, and a hydrogen and methanol selling price of 5 €/kg and 500 €/t, respectively. The electrolyzer replacement cost is included in the electrolyzer CAPEX, and the heat pump cost is included in the heat recovery CAPEX.

| Parameter	Unit	S-M-EL	S–H–S	S–P–S	S-M-COEL	D-M-EL	D-H-R	D-P-R
LCOM/ LCOH	€/t_{MeOH}-kg_{H2}	502.84	2.32		504.00	281.92	1.11	
NPV	M€	−25.70	131.70	0.07	−17.62	135.47	282.80	87.98
IRR	%	8%	45%	8%	10%	29%	73%	73%
CAPEX Total	M€	40.77	38.07	17.16	40.04	123.60	45.91	14.18
CAPEX Depreciation	M€/y	4.15	3.88	1.75	4.08	12.59	4.68	14.18
CAPEX Heat recovery	M€	7.06	6.98	11.53	7.20	12.72	8.25	
CAPEX Electrolyzer	M€	21.02	25.45		20.09	76.56	37.66	
CAPEX Methanol synthesis	M€	8.97			9.03	34.32		
CAPEX CO_2 purification	M€	3.72	5.64	5.64	3.72			
Net Cash Flow	M€/y	4.10	17.29	1.76	4.73	35.72	33.48	10.40
Electricity Purchasing Cost	M€/y	7.72	8.87	−0.16	7.21	29.47	12.64	−0.70
O&M Cost	M€/y	0.82	0.76	0.34	0.80	2.47	0.92	0.28
CO_2 management costs	M€/y			0.83	0.83			
CO-rich gas management	M€/y						4.74	4.74
Revenue from MeOH	M€/y	9.90			9.99	53.02		
Revenue from H_2	M€/y	0.00	24.99				37.05	
Revenue from CO2 tax	M€/y	2.73	2.77	2.77	2.75	14.64	14.72	14.72

Table 8

Costs and revenues of the different case studies for the short-term scenario, with an electrolyzer cost of 1000 €/kW$_{el}$, an electricity cost of 100 €/MWh, and a hydrogen and methanol selling price of 3 €/kg and 400 €/t, respectively. 'NA' stands for 'not available' when the net cash flow is negative and the *IRR* cannot be calculated. The electrolyzer replacement cost is included in the electrolyzer CAPEX, and the heat pump cost is included in the heat recovery CAPEX.

Parameter	Unit	S-M-EL	S–H–S	S–P–S	S-M-COEL	D-M-EL	D-H-R	D-P-R
LCOM/ LCOH	€/t$_{MeOH}$-kg$_{H2}$	1022.23	4.71		987.03	647.82	3.44	
NPV	M€	−120.99	−84.00	1.67	−107.99	−258.01	−31.86	94.90
IRR	%	NA	NA	9%	NA	NA	2%	78%
CAPEX Total	M€	61.80	63.52	17.16	60.13	200.16	83.57	14.18
CAPEX Depreciation	M€/y	6.29	6.47	1.75	6.12	20.39	8.51	1.44
CAPEX Heat recovery	M€	7.06	6.98	11.53	7.20	12.72	8.25	14.18
CAPEX Electrolyzer	M€	42.05	50.90		40.18	153.11	75.31	
CAPEX Methanol synthesis	M€	8.97			9.03	34.32		
CAPEX CO$_2$ purification	M€	3.72	5.64	5.64	3.72			
Net Cash Flow	M€/y	−6.03	−2.09	1.92	−4.87	−5.89	5.27	11.11
Electricity Purchasing Cost	M€/y	15.45	17.75	−0.32	14.41	58.95	25.28	−1.41
O&M Cost	M€/y	1.24	1.27	0.34	1.20	4.00	1.67	0.28
CO$_2$ management costs	M€/y		0.83	0.83				
CO-rich gas management	M€/y						4.74	4.74
Revenue from MeOH	M€/y	7.92			7.99	42.42		
Revenue from H$_2$	M€/y		14.99				22.23	
Revenue from CO$_2$ tax	M€/y	2.73	2.77	2.77	2.75	14.64	14.72	14.72

(a)   (b)
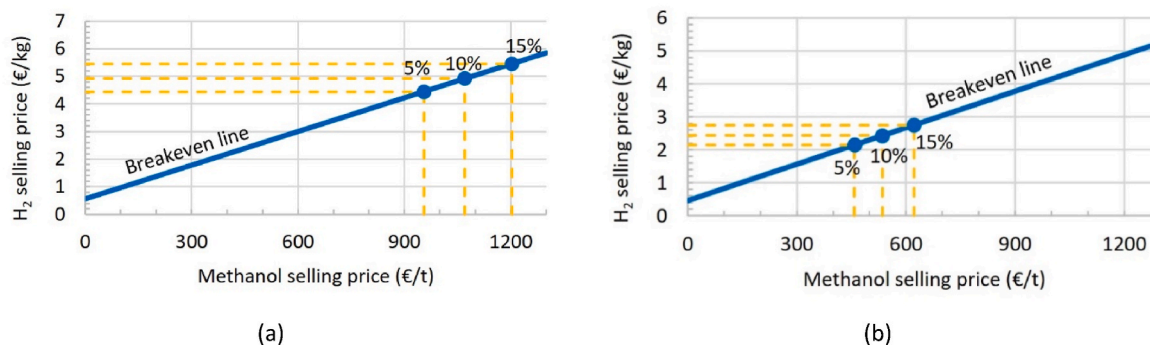
Fig. 5. Hydrogen-methanol selling price breakeven line and iso-IRR lines for cases S–H–S and S-M-EL for electrolyzer and electricity costs of (a) 1000 €/kW and 100 €/MWh, and (b) 500 €/kW and 50 €/MWh. The breakeven line identifies the regions that make hydrogen production with S–H–S plant more competitive (above the line) or methanol production with S-M-EL plant more competitive (below the line).

(a)   (b)
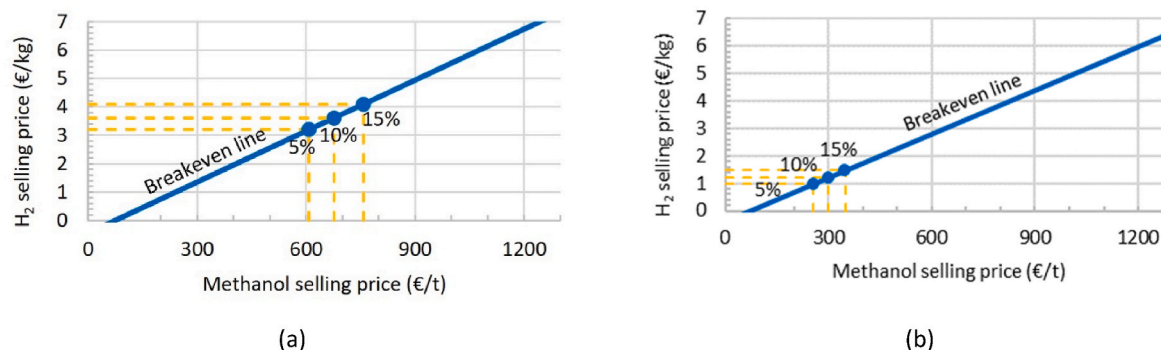
Fig. 6. Hydrogen-methanol selling price breakeven line and iso-IRR lines for cases D-H-R and D-M-EL for electrolyzer and electricity costs of (a) 1000 €/kW$_{el}$ and 100 €/MWh, and (b) 500 €/kW$_{el}$ and 50 €/MWh. The breakeven line identifies the regions that make hydrogen production with D-H-R plant more competitive (above the line) or methanol production with D-M-EL plant more competitive (below the line).

steel premium of around 15, 40, and 60 €/t for scrap-fed EAF cases as well as a steel premium of 0, 20, and 40 €/t for DRI-fed EAF cases are needed when the electricity cost is 50, 100, and 150 €/MWh, respectively. Fig. 9 shows that for a breakeven hydrogen selling price of 3 €/kg, a steel premium of around 0, 25, and 55 €/t for scrap-fed EAF cases as well as a steel premium with negative, 2, and 13 €/t for DRI-fed EAF cases are needed when the electricity cost is 50, 100, and 150 €/MWh, respectively. The effect of the electricity cost for case D-M-EL is lower with respect to case S-M-EL, due to the lower amount of electricity

needed per ton of steel in the DRI-fed EAF case.

6. Limits of the study

The present work is affected by the limitations listed here, which may be addressed by future investigations.

- The work is based on steady-state balances evaluated on average values of flow rates and composition. More in-depth studies may
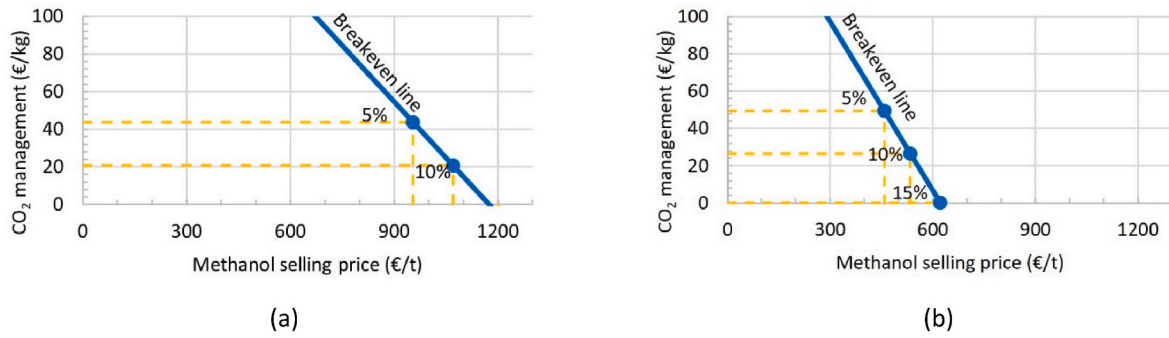
Fig. 7. CO_2 management costs-methanol selling price breakeven line and iso-IRR lines for cases S–P–S and S-M-EL for electrolyzer and electricity costs of (a) 1000 €/kW$_{el}$ and 100 €/MWh, and (b) 500 €/kW$_{el}$ and 50 €/MWh. The breakeven line identifies the regions that make case S–P–S with sole CO_2 capture more competitive (below the line) or methanol production with S-M-EL plant more competitive (above the line).
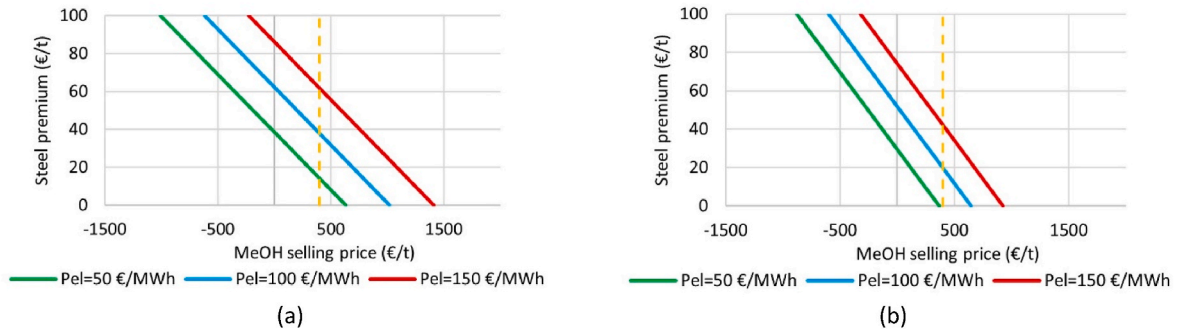

Fig. 8. Steel premium and methanol breakeven price for electricity prices of 50, 100 and 150 €/MWh, for case study S-M-EL (a) and D-M-EL (b) with an electrolysis cost of 1000 €/kW.
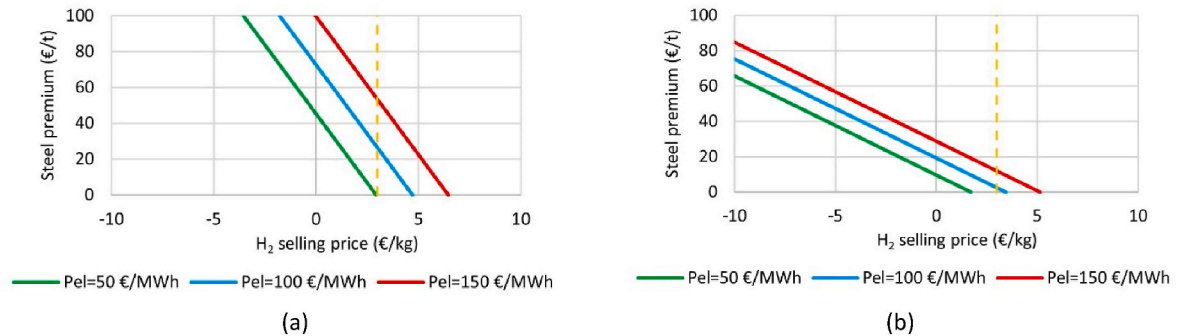

Fig. 9. Steel premium and hydrogen breakeven price for electricity prices of 50, 100 and 150 €/MWh, for case study S–H–S (a) and D-H-R (b) with an electrolysis cost of 1000 €/kW.

consider the effect of the variability of these quantities, which would require the adoption of off-design and dynamic models.

- Integration with the DRI production process to which hydrogen or CO-rich gas can be exported has been evaluated in a simplified way. Greater accuracy would be achieved by calculating the mass and energy balances of the EAF process integrated with DRI production plants. This more detailed study would need though a revised approach for the calculation of the levelized cost of the products with respect to the one proposed in this work.

- Data on the properties of gases without postcombustion were derived from a model that minimizes false air leakage and considers complete oxygen consumption. These conditions require validation on an industrial scale, which at the moment cannot be performed due to the lack of plants of this type on the market.

7. Conclusions

The main goal of this study is to perform a techno-economic analysis of chimneyless electric arc furnace plants, fed by either scrap or DRI, for the coproduction of steel and of electricity, hydrogen, or methanol. In the new plant, the EAF is characterized by decreased false air leakage and by heat recovery for steam production; in addition, a combination of the following components is integrated: oxy-postcombustion, carbon capture, CO-rich gas recovery, hydrogen or syngas production by high-temperature electrolysis or coelectrolysis, and methanol synthesis. Thus, this study specifically addresses the efficient management of the EAF exhaust gas to investigate and compare different decarbonization options of the EAF route in steelmaking. The main conclusions from this work are synthesized as follows.

- The specific net electric power input of the plants including an electrolysis system, i.e. those involving the production of hydrogen or methanol, ranges from 235 to 649 kWh/t$_{steel}$, and hence it has the same order of magnitude as the electricity consumed in the EAF steel melting process, which is about 350 kWh/t$_{steel}$. The specific net electric power input in the DRI-fed e-methanol case is lower than in the corresponding scrap-fed case, due to the absence of post-combustion in the DRI-fed EAF plant, which allows to produce methanol from a CO–H$_2$ stream rather than from a CO$_2$–H$_2$ mixture.

- All cases allow achieving a substantial reduction of direct carbon dioxide emissions, with about 99% avoidance compared to the un-abated conditions, attained either via carbon capture and storage or via carbon capture and utilization.

- In a long-term scenario, with low electrolysis and electricity costs, high hydrogen and methanol selling prices, the internal rate of return varies between 8 and 45% for the scrap-fed cases and between 29 and 73% for the DRI-fed case. In a short-term scenario, only case studies S–P–S, D-H-R, and D-P-R are economically competitive, with an *IRR* of 9%, 2% and 78%, respectively. Plants based on power generation and carbon capture and storage (S–P–S and D-P-R) are insensitive to the variation of the electricity cost.

- The production and sale of hydrogen and methanol is competitive with market prices only for low electricity costs. When the electricity cost is high, the case S–P–S is more competitive than the case S-M-EL.

- In a low electricity cost (50 €/MWh) scenario, with a methanol selling price of 500 €/t, the scrap-fed EAF CCU case is more economically competitive than the scrap-fed EAF CCS case only for relatively high carbon dioxide management costs above 40 €/t. In the higher electricity cost scenario (100 €/MWh), the CCS case is more competitive than the CCU case, except for extremely high CO$_2$ management costs, above 100 €/t.

- For a methanol selling price of 400 €/t, a steel premium of 15, 40, and 60 €/t for scrap-fed EAF cases as well as of 0, 20 and 40 €/t for DRI-fed EAF cases are needed when the electricity cost is 50, 100, and 150 €/MWh, respectively. Also, for a hydrogen selling price of 3 €/kg, a steel premium of 0, 25, and 55 €/t for scrap-fed EAF cases as well as with negative, 2, and 13 €/t for DRI-fed EAF cases are needed when the electricity cost is 50, 100, and 150 €/MWh, respectively. The values of the steel premium are acceptable, considering a cost of steel of 500 €/t.

In short, the novel proposed chimneyless electric arc furnaces result to be technically and economically promising options to reduce carbon dioxide emissions. The configurations of DRI-fed furnaces result more competitive with respect to scrap-fed furnaces, while the competitiveness of sole electricity, hydrogen, or methanol production configurations depends on the case study analyzed and, more importantly, on future market prices.

CRediT authorship contribution statement

Camilla Nicol Bonacina: Writing – original draft, Visualization, Validation, Software, Methodology, Investigation, Formal analysis, Data curation, Conceptualization. **Matteo Carmelo Romano:** Writing – review & editing, Visualization, Supervision, Methodology, Formal analysis, Conceptualization. **Paolo Colbertaldo:** Writing – review & editing, Methodology, Investigation, Formal analysis. **Alessio Milocco:** Writing – review & editing, Data curation. **Gianluca Valenti:** Writing – review & editing, Supervision, Project administration, Methodology, Formal analysis, Conceptualization.

Declaration of competing interest

The authors declare that they have no known competing financial interests or personal relationships that could have appeared to influence the work reported in this paper.

Data availability

Data will be made available on request.

Nomenclature

Acronyms

CCS	Carbon capture and storage
CCU	Carbon capture and utilization
EAF	Electric arc furnace
EL	Electrolyzer
MeOH	Methanol
O&M	Operation and maintenance
SOEC	Solid oxide electrolysis

Symbols

η	Efficiency, -
C	Cost, € or €/year
CF	Indirect cost factor, %
EC	Equipment cost, €
F	Faraday's constant, C
H	Hours of operation
ICF	Installation cost factor, %
J	Current density, A/cm^2
k	Thermal power loss constant, kW/(Nm$^3_{CO,CO2}$/h)
IRR	Internal rate of return, %
$LCOH$	Levelized cost of hydrogen, €/kg
$LCOM$	Levelized cost of methanol, €/t
LHV	Lower Heating Value, W/kg
LT	Lifetime, years
$\dot{m}$	Mass flow rate, g/s
N	Number, -

$\dot{n}$	Mole flow rate, mol/s
NCF	Net cash flow, €/year
NPV	Net present value, €
P	Price, €/kg or scaling factor, -
$\dot{Q}$	Thermal power, W
R	Revenue, €/year
r	Discount rate, -
RR	Recycle ratio, -
RU	Reactant utilization factor, -
S	Surface, m^2 or scaling parameter
V	Voltage, V
$\dot{V}$	Volume flow rate, m^3/s
$\dot{W}$	Power, W

Subscripts

comb	Combustion
el	Electric
exc	Excess
exh	Exhaust
inv	Investment
prod	Products
R	Reactor
react	Reactants
ref	Reference
rep	Replacement
var	Variable
y	Yearly

Appendix A. Supplementary data

Supplementary data to this article can be found online at https://doi.org/10.1016/j.jclepro.2024.143048.

References

Abad, D., Vega, F., Navarrete, B., Delgado, A., Nieto, E., 2021. Modeling and simulation of an integrated power-to-methanol approach via high temperature electrolysis and partial oxy-combustion technology. Int. J. Hydrogen Energy 46 (69), 34128–34147. https://doi.org/10.1016/j.ijhydene.2021.04.029.

Andersson, J., Grönkvist, S., 2022. Improving the economics of fossil-free steelmaking via co-production of methanol. J. Clean. Prod. 350, 131469 https://doi.org/10.1016/j.jclepro.2022.131469.

Arpagaus, C., 2021. Industrial Heat Pumps: Market Overview and Applications.

Bailera, M., Lisbona, P., Peña, B., Romeo, L.M., 2021. A review on CO2 mitigation in the Iron and Steel industry through Power to X processes. J. CO2 Util. 46, 101456 https://doi.org/10.1016/j.jcou.2021.101456.

Blumberg, T., Tsatsaronis, G., Morosuk, T., 2019. On the economics of methanol production from natural gas. Fuel 256, 115824. https://doi.org/10.1016/j.fuel.2019.115824.

Chemical Engineering, 2024. Plant Cost Index. Https://Www.Chemengonline.Com/Site/Plant-Cost-Index/.

Clean Air Task Force, 2023. Solid Oxide Electrolysis: A Technology Status Assessment.

CLEANKER, 2017. Clean Clinker Production via Calcium Looping Process, D5.10.

Crespi, E., Colbertaldo, P., Guandalini, G., Campanari, S., 2021. Design of hybrid power-to-power systems for continuous clean PV-based energy supply. Int. J. Hydrogen Energy 46 (26), 13691–13708. https://doi.org/10.1016/j.ijhydene.2020.09.152.

Danieli, & Tenova, 2024. ENERGIRON. DRI Technology by Tenova and Danieli. Https://Www.Energiron.Com.

d'Amore, F., Nava, A., Colbertaldo, P., Visconti, C.G., Romano, M.C., 2023. Turning CO2 from fuel combustion into e-Fuel? Consider alternative pathways. Energy Convers. Manag. 289, 117170 https://doi.org/10.1016/j.enconman.2023.117170.

d'Amore, F., Natalucci, L., Romano, M.C., 2024. Optimisation of ship-based CO2 transport chains from Southern Europe to the North Sea. Carbon Capture Science & Technology 10, 100172. https://doi.org/10.1016/j.ccst.2023.100172.

Gatti, M., Martelli, E., Di Bona, D., Gabba, M., Scaccabarozzi, R., Spinelli, M., Viganò, F., Consonni, S., 2020. Preliminary performance and cost evaluation of Four alternative technologies for Post-combustion CO2 capture in natural gas-Fired power plants. Energies 13 (3), 543. https://doi.org/10.3390/en13030543.

Hong, J., Chaudhry, G., Brisson, J.G., Field, R., Gazzino, M., Ghoniem, A.F., 2009. Analysis of oxy-fuel combustion power cycle utilizing a pressurized coal combustor. Energy 34 (9), 1332–1340. https://doi.org/10.1016/j.energy.2009.05.015.

Hub, N.C., 2024. North-C-Methanol. Https://Northccuhub.Eu/North-c-Methanol/.

International Energy Agency, 2019a. Global Average Levelised Cost of Hydrogen Production by Energy Source and Technology, 2019 and 2050.

International Energy Agency, 2019b. Putting Carbon Dioxide to Use.

International Energy Agency, 2021. Energy Efficiency.

Kirschen, M., Risonarta, V., Pfeifer, H., 2009. Energy efficiency and the influence of gas burners to the energy related carbon dioxide emissions of electric arc furnaces in steel industry. Energy 34 (9), 1065–1072. https://doi.org/10.1016/j.energy.2009.04.015.

Kiss, A.A., Pragt, J.J., Vos, H.J., Bargeman, G., de Groot, M.T., 2016. Novel efficient process for methanol synthesis by CO 2 hydrogenation. Chem. Eng. J. 284, 260–269. https://doi.org/10.1016/j.cej.2015.08.101.

Leonzio, G., Zondervan, E., Foscolo, P.U., 2019. Methanol production by CO2 hydrogenation: analysis and simulation of reactor performance. Int. J. Hydrogen Energy 44 (16), 7915–7933. https://doi.org/10.1016/j.ijhydene.2019.02.056.

Magli, F., Spinelli, M., Fantini, M., Romano, M.C., Gatti, M., 2022. Techno-economic optimization and off-design analysis of CO2 purification units for cement plants with oxyfuel-based CO2 capture. Int. J. Greenh. Gas Control 115, 103591. https://doi.org/10.1016/j.ijggc.2022.103591.

Marocco, P., Gandiglio, M., Audisio, D., Santarelli, M., 2023. Assessment of the role of hydrogen to produce high-temperature heat in the steel industry. J. Clean. Prod. 388, 135969 https://doi.org/10.1016/j.jclepro.2023.135969.

Methanol Institute, 2024. Methanol Price and Supply/Demand. Https://Www.Methanol.Org/Methanol-Price-Supply-Demand/.

Minutillo, M., Perna, A., Forcina, A., Di Micco, S., Jannelli, E., 2021. Analyzing the levelized cost of hydrogen in refueling stations with on-site hydrogen production via water electrolysis in the Italian scenario. Int. J. Hydrogen Energy 46 (26), 13667–13677. https://doi.org/10.1016/j.ijhydene.2020.11.110.

Pérez-Fortes, M., Schöneberger, J.C., Boulamanti, A., Tzimas, E., 2016. Methanol synthesis using captured CO2 as raw material: techno-economic and environmental assessment. Appl. Energy 161, 718–732. https://doi.org/10.1016/j.apenergy.2015.07.067.

Pratschner, S., Radosits, F., Ajanovic, A., Winter, F., 2023. Techno-economic assessment of a power-to-green methanol plant. J. CO2 Util. 75, 102563 https://doi.org/10.1016/j.jcou.2023.102563.

Rubin, E.S., Davison, J.E., Herzog, H.J., 2015. The cost of CO2 capture and storage. Int. J. Greenh. Gas Control 40, 378–400. https://doi.org/10.1016/j.ijggc.2015.05.018.

Shahabuddin, M., Brooks, G., Rhamdhani, M.A., 2023. Decarbonisation and hydrogen integration of steel industries: Recent development, challenges and technoeconomic analysis. J. Clean. Prod. 395, 136391 https://doi.org/10.1016/j.jclepro.2023.136391.

Smolinka, T., Ojong, E.T., Garche, J., 2015. Hydrogen production from Renewable Energies—electrolyzer technologies. In: Electrochemical Energy Storage for Renewable Sources and Grid Balancing. Elsevier, pp. 103–128. https://doi.org/10.1016/B978-0-444-62616-5.00008-5.

SSAB, L. & V, 2024. HYBRIT. Https://Www.Hybritdevelopment.Se/En/.

Sunfire, 2024. Hydrogen. Https://Www.Sunfire.de/En/Hydrogen.

TBU, 2024. Methanol Plant. Https://Www.Tbu.No/En/Ressurser/.

Waidhas, M., Wegener, D., 2011. Method and Device for Using Emissions from an Industrial Installation. Patent WO2011101217A2).

Wang, R.R., Zhao, Y.Q., Babich, A., Senk, D., Fan, X.Y., 2021. Hydrogen direct reduction (H-DR) in steel industry—an overview of challenges and opportunities. J. Clean. Prod. 329, 129797 https://doi.org/10.1016/j.jclepro.2021.129797.

World Steel Association, 2022. About Steel. Https://Worldsteel.Org/.